

Light scattering properties for spherical and cylindrical particles: a simple approximation derived from Mie calculations

Tatiana A. Bashkatova, Alexey N. Bashkatov, Vyacheslav I. Kochubey, Valery V. Tuchin

Saratov State University, Astrakhanskaya 83, Saratov 410026, Russia

ABSTRACT

The scattering cross section and asymmetry factor g are important parameters to describe light propagation in turbid media. We present simple approximation for these parameters derived from Mie calculations within wide range of values of the size parameter x and relative refractive index m .

Keywords: light scattering, Mie theory approximation, light propagation modeling

1. INTRODUCTION

Simulations of light propagation in turbid media with scattering and partly absorbing particles having shape of cylinder or sphere which are similar to shape of the scatterers in living tissues, can be performed by using Monte Carlo simulations [1, 2] or the transport theory [3, 4]. The basic properties of the scatterers, such as σ_a and σ_s , the absorption and scattering cross sections, respectively, and g the asymmetry factor, which is the average cosine of the scattering angle, must be known.

The rigorous formulas in Mie theory are series on multipolar number n . Such representation is very inconvenient in the practical applications and more simple approximating formulas are often used instead of them. Usually, the range of applicability of these approaches is not wide and depends on the value of the size parameter $x = ka$, where k – wavenumber of an incident wave, a – radius of a particle. Therefore, to simulate a light propagation through the turbid media it is necessary to use numerical calculations based on the formulas of Mie theory, or to use approximating methods of calculations which yield a considerable error outside of their applicability.

In this study the simple analytical formulas which allow to substitute the formulas of Mie theory without considerable sacrifice of accuracy of calculations are presented.

2. MIE SCATTERING FOR A SINGLE SPHERE AND SINGLE CYLINDER

Values of scattering cross section can be derived for single spherical or infinite cylindrical particles which are illuminated by a plane wave by using Mie theory [5]. The scattered field is determined by the size parameter $x = 2\pi a/\lambda$, where a and λ represent the radius of the particle and the wavelength in the surrounding medium, respectively, and by m , the ratio of the refractive indices of the particle and surrounding medium. Absorption by the spherical and cylindrical particles can be considered as well in Mie theory. However, it is not taken into account in our study. Our results have been obtained with Mie scattering computer program based on the program reported by Bohren and Huffman [5], running on a personal computer with a coprocessor.

2.1 Mie scattering for a single sphere

The problem of sphere with arbitrary radius and refractive index is the most important and precisely solved in the theory of light absorption and scattering by small particles. Though the formal solution of this problem is well-known, for calculations it began to be applied only with appearance of modern computers.

Address all correspondence to Alexey N. Bashkatov. Tel: 8452 514693; E-mail: bash@optics.sgu.ru

Cross section of the scattering by sphere illuminated by non polarized light represented in Ref. [5]. It is defined by:

$$\sigma_s = \frac{2\pi}{k^2} \sum_{n=1}^{\infty} (2n+1) (|a_n|^2 + |b_n|^2).$$

where $k = \frac{2\pi}{\lambda} n_l$ is the wavenumber; λ is the wavelength of light; n_l is the real part of refractive index of the medium which surrounds the scattering particle; a_n and b_n - expansion coefficients of a scattering electromagnetic field on vector spherical harmonics (scattering series).

$$a_n = \frac{m\psi_n(mx)\psi'_n(x) - \psi_n(x)\psi'_n(mx)}{m\psi_n(mx)\xi'_n(x) - \xi_n(x)\psi'_n(mx)}$$

$$b_n = \frac{\psi_n(mx)\psi'_n(x) - m\psi_n(x)\psi'_n(mx)}{\psi_n(mx)\xi'_n(x) - m\xi_n(x)\psi'_n(mx)},$$

where $m = \frac{n_s}{n_l}$ is the relative refractive index; n_s is the real part of refractive index of the scattering particle;

$x = ka = \frac{2\pi n_l a}{\lambda}$ is the size parameter; a is the radius of scattering particle;

$\psi_n(\rho) = \rho J_n(\rho)$, $\xi_n(\rho) = \rho H_n^{(1)}(\rho)$ is the Riccati-Bessel functions; $J_n(\rho)$ is the Bessel function of the 1-st kind of n -order; $H_n^{(1)}(\rho)$ is the Bessel function of the 3-rd kind of n -order.

Asymmetry factor of light scattering by the spherical particle g (the average cosine of scattering angle) is defined by [5]

$$g = \langle \cos \theta \rangle = \frac{4}{x^2 Q_s} \left[\sum_n \frac{n(n+2)}{n+1} \operatorname{Re} \{ a_n a_{n+1}^* + b_n b_{n+1}^* \} + \sum_n \frac{2n+1}{n(n+1)} \operatorname{Re} \{ a_n b_n^* \} \right]$$

where a_n, b_n, a_n^*, b_n^* are the coefficients and complex conjugate to them of scattering series, (sign * denotes complex conjugation); $Q_s = \frac{\sigma_s}{\pi a^2}$ is the efficiency factor of the scattering.

2.2 Mie scattering for a single cylinder

Fibrous tissues have a structure formed by collagen fibers and bundles of the collagen fibers [6, 7]. Examples of these tissues are the connective tissues, a cornea and sclera of an eye etc. These scatterers are described in the best way as cylinders with size much more than their diameter.

Consider the infinite cylinder of radius a on which the plane homogeneous wave is incident and formed angle ζ with the axis of cylinder. It is possible two polarization of incident wave: 1) Electric field is parallel to the plane which is perpendicular to the axis of cylinder and 2) Electric field is parallel to the axis of cylinder.

Case 1. Electric field is parallel to the plane which is perpendicular to the axis of cylinder.

The coefficients of scattering series in this case [5]:

$$\begin{aligned}
a_{nl} &= \frac{C_n V_n - B_n D_n}{W_n V_n + i D_n^2}, & b_{nl} &= \frac{W_n B_n + i D_n C_n}{W_n V_n + i D_n^2} \\
D_n &= n \cos \zeta \eta J_n(\eta) H_n^{(1)}(\xi) \left(\frac{\xi^2}{\eta^2} - 1 \right), \\
B_n &= \xi \left[m^2 \xi J_n'(\eta) J_n(\xi) - \eta J_n(\eta) J_n'(\xi) \right], \\
C_n &= n \cos \zeta \eta J_n(\eta) J_n(\xi) \left(\frac{\xi^2}{\eta^2} - 1 \right), \\
V_n &= \xi \left[m^2 \xi J_n'(\eta) H_n^{(1)}(\xi) - \eta J_n(\eta) H_n^{(1)'}(\xi) \right], \\
W_n &= i \xi \left[\eta J_n(\eta) H_n^{(1)'}(\xi) - \xi J_n'(\eta) H_n^{(1)}(\xi) \right], \\
\xi &= x \sin(\zeta), & \eta &= x \sqrt{m^2 - \cos^2(\zeta)}.
\end{aligned}$$

If incident field is perpendicular to the axis of cylinder ($\zeta = 90^\circ$), the coefficient a_{nl} turn to zero,

$$b_{nl}(\zeta = 90^\circ) = b_n = \frac{J_n(mx) J_n'(x) - m J_n'(mx) J_n(x)}{J_n(mx) H_n^{(1)'}(x) - m J_n'(mx) H_n^{(1)}(x)}$$

In this case the efficiency factor of the scattering defined by following expression:

$$Q_{sl} = \frac{2}{x} \left[|b_{0l}|^2 + 2 \sum_{n=1}^{\infty} (|b_{nl}|^2 + |a_{nl}|^2) \right]$$

Case II. Electric field is parallel to the axis of cylinder

The coefficients of scattering series in this case [5].

$$\begin{aligned}
a_{nll} &= -\frac{A_n V_n - i C_n D_n}{W_n V_n + i D_n^2}, & b_{nll} &= -i \frac{C_n W_n + A_n D_n}{W_n V_n + i D_n^2} \\
A_n &= i \xi \left[\xi J_n'(\eta) J_n(\xi) - \eta J_n(\eta) J_n'(\xi) \right]
\end{aligned}$$

If incident field is perpendicular to the axis of cylinder, then b_{nll} turn to zero,

$$a_{nll}(\zeta = 90^\circ) = a_n = \frac{m J_n(mx) J_n'(x) - J_n'(mx) J_n(x)}{m J_n(mx) H_n^{(1)'}(x) - J_n'(mx) H_n^{(1)}(x)}$$

In this case the efficiency factor of the scattering defined by:

$$Q_{sII} = \frac{2}{x} \left[|a_{0II}|^2 + 2 \sum_{n=1}^{\infty} (|a_{nII}|^2 + |b_{nII}|^2) \right]$$

If incident light is non polarized, the efficiency factor are equal.

$$Q_s = \frac{Q_{sI} + Q_{sII}}{2}$$

Asymmetry factor of light scattering g (average cosine of scattering angle) for the case of the infinite cylinder illuminated by non polarized light is defined by following relation:

$$g = \langle \cos \theta \rangle = \frac{\int_0^{\pi} \frac{T_{11}}{T_{11norm}} \cos(\theta) \sin(\theta) d\theta}{\int_0^{\pi} \frac{T_{11}}{T_{11norm}} \sin(\theta) d\theta}$$

$$T_{11} = \frac{|T_1|^2 + |T_2|^2}{2}, \quad T_{11norm} = \frac{|b_{0I} + 2b_{nI} \cos \theta|^2 + |a_{0II} + 2a_{nII} \cos \theta|^2}{2}$$

$$T_1 = b_{0I} + 2 \sum_{n=1}^{\infty} b_{nI} \cos(n\theta),$$

$$T_2 = a_{0II} + 2 \sum_{n=1}^{\infty} a_{nII} \cos(n\theta),$$

T_1 и T_2 – components of the amplitude forward scattering matrix; T_{11} - component of the scattering matrix [5].

3. APPROXIMATION FOR CASE OF THE SINGLE SPHERE AND THE SINGLE CYLINDER

As was mentioned above, the aim of this study is to find simple formulas for performing estimating calculations of optical parameter of tissues. Moreover, essential dispersion of the optical parameters in the tissues narrowing down the high accuracy of calculations, given of the Mie theory.

The most of scatterers in tissues have the shape similar to sphere (cells of an epidermis, cells of a fat layer, the erythrocytes of a blood etc.) or have the cylindrical shape (fibers of connective tissue, sclera and cornea of an eye, *dura mater* etc.). In this connection to describe an optical properties of most types of the tissues with needed for practical calculation accuracy it is enough to consider two types of scatterers: sphere and infinite cylinder.

To find approximating functions we aspired to avoid using of special functions, and to use simple analytical expressions as far as possible. We have made an attempt to consider the wide range of Q_s and g . We have considered a range from 1 to 1.5 and from 0 to 50 for m and x , respectively.

3.1 Approximation for case of the single spherical particle

3.1.1 Efficiency factor of the scattering for single spherical particle

Consider the efficiency factor of the scattering for the case of the single spherical particle. Figs. 1-5 show complicated nonlinear behavior of dependence Q_s on size parameter x and relative refractive index m . Unfortunately, we did not find the uniform function to describe dependence $Q_s = Q_s(m, x)$ for investigated ranges of m and x .

For x from 0 to $\frac{2.5869243m}{-0.99524473 + m}$,

$$Q_s(m, x) = \frac{A + Bx}{1 + Cx + Dx^2} \quad (1)$$

where

$$\begin{aligned} A &= \frac{-0.069144178 + 0.046660396m}{1 - 1.0294684m + 0.23995219m^2} \\ B &= -0.808706 + 0.81953333m \\ C &= 0.86969218 - 0.86159152m \\ D &= 0.098773091 + 0.098543877 \cdot \cos(2.4950934m + 0.6149086) \end{aligned}$$

For x from $\frac{2.5869243m}{-0.99524473 + m}$ to 50,

$$Q_s(m, x) = A \exp(-Bx) \cdot \sin(Cmx + D) + 0.11m + 2.1 \quad (2)$$

where

If $m > 1$ and $m \leq 1.25$

$$A = -31.81595 + 53.5842m - 21.904m^2$$

Otherwise

$$A = 22.7013 - 11.329513m - \frac{15.054382}{m^2}$$

$$B = -25.310148 + 72.090822m - 76.476191m^2 + 35.816934m^3 - 6.2379578m^4$$

$$C = 1.9733402 - \frac{1.965552}{m}$$

If $m > 1$ and $m \leq 1.3$

$$D = \frac{319588481.0 + 45.479092 \cdot m^{61.248596}}{105397580.0 + m^{61.248596}}$$

Otherwise

$$D = 0.28194245 - 3.2273766 \cdot \exp(-0.045910896 \cdot m^{14.552944})$$

Solving of this problem is connected with splitting of the range definition of function in two parts. The first one is described by the simple rational function (Eq. 1). Coefficients and its analytical expressions (as a function from m) were obtained for each value of m .

The second part of dependence Q_s on size parameter x is described by function, similar to one, which describes the damped vibration of oscillator. It was modified a little by us (Eq. 2). Figs. 1-5 show that approximation offered by us in a good agreement with a rigorous solution obtained by Mie theory.

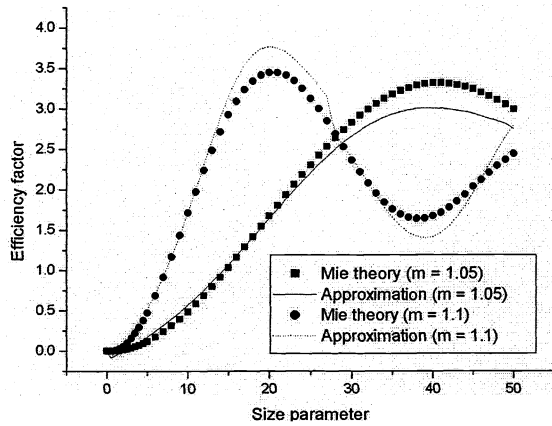


Figure 1. Efficiency factor for Mie scattering of non absorbing spheres as a function of size parameter x and relative refractive index m (symbols). The solid and dashed curves represent the predictions of Eqs. 1 and 2.

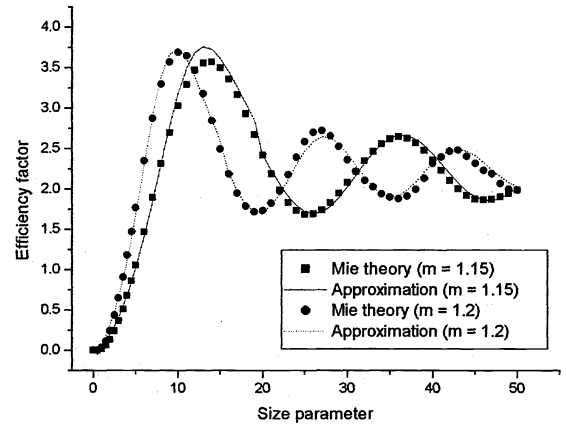


Figure 2. Efficiency factor for Mie scattering of non absorbing spheres as a function of size parameter x and relative refractive index m (symbols). The solid and dashed curves represent the predictions of Eqs. 1 and 2.

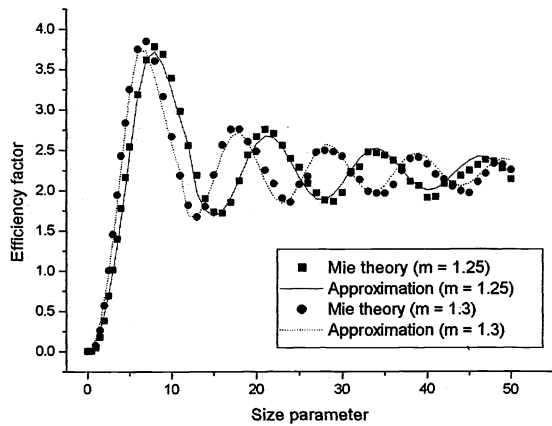


Figure 3. Efficiency factor for Mie scattering of non absorbing spheres as a function of size parameter x and relative refractive index m (symbols). The solid and dashed curves represent the predictions of Eqs. 1 and 2.

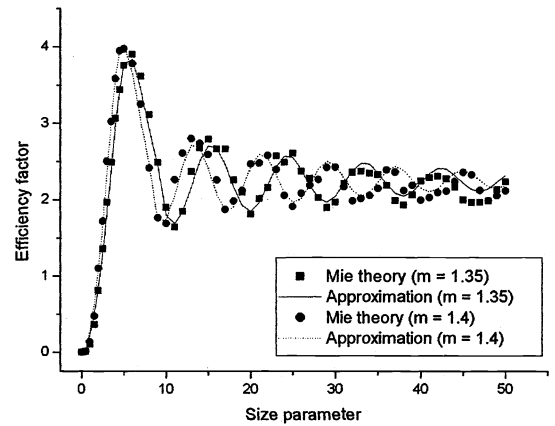


Figure 4. Efficiency factor for Mie scattering of non absorbing spheres as a function of size parameter x and relative refractive index m (symbols). The solid and dashed curves represent the predictions of Eqs. 1 and 2.

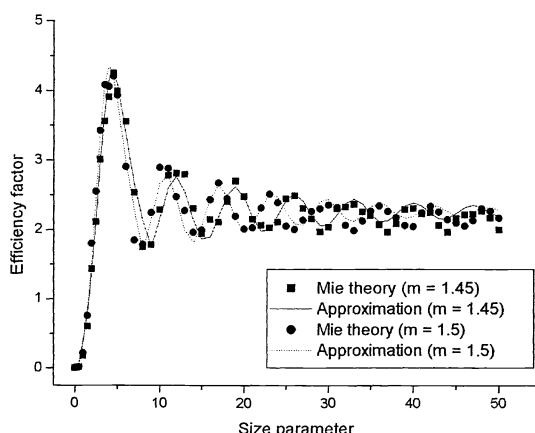


Figure 5. Efficiency factor for Mie scattering of non absorbing spheres as a function of size parameter x and relative refractive index m (symbols). The solid and dashed curves represent the predictions of Eqs. 1 and 2.

3.1.2 Asymmetry factor for the case of the single spherical particle

Similar approach is used for approximation construction to calculate the asymmetry factor (Eqs. 3, 4). Obtained results are shown in Figs. 6-10. From these figures it is seen that the accuracy of approximating solution is smaller than in a case of approximating Q_s , especially for high values of m and x (Figs. 6-10). Nevertheless, approximation formulas offered by us predict qualitatively correctly the asymmetry factor dependence on size parameter and relative refractive index.

For x from 0 to $58.48979 - 49.978127 \cdot \exp(-3.7264027 \cdot m^{-14.934118})$,

$$g(m, x) = \frac{A + Bx}{1 + Cx + Dx^2} \quad (3)$$

where

$$A = \frac{1}{-40.482625 + 73.261124m - 39.846712m^2}$$

$$B = 0.81888008 \cdot m^{-2.7909634}$$

$$C = -2.2733334 + \frac{3.0165848}{m}$$

$$D = 0.56374493 - 1.2787749m + 0.86720047m^2 - 0.15106449m^3$$

For x from $58.48979 - 49.978127 \cdot \exp(-3.7264027 \cdot m^{-14.934118})$ to 50

$$g(m, x) = A + Bx + \frac{C}{x^2} \quad (4)$$

where

$$A = 0.91235911 - 0.19992982 \cdot \exp(-260.07022 \cdot m^{-16.719608})$$

$$B = 5.8635545 - 24.754781m + 41.600981m^2 - 34.741271m^3 + 14.404556m^4 - 2.3709316m^5$$

$$C = \frac{-5.1260456 + 3.255653m}{1 - 1.4956858m + 0.57640499m^2}$$

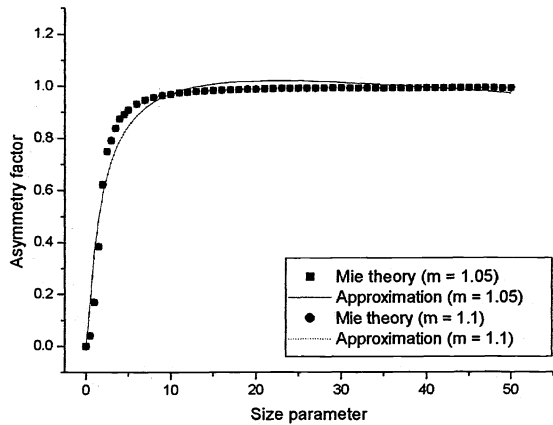


Figure 6. Average cosine of the scattering angle g for Mie scattering of non absorbing spheres as a function of size parameter x and relative refractive index m (symbols). The solid and dashed curves represent the predictions of Eqs. 3 and 4.

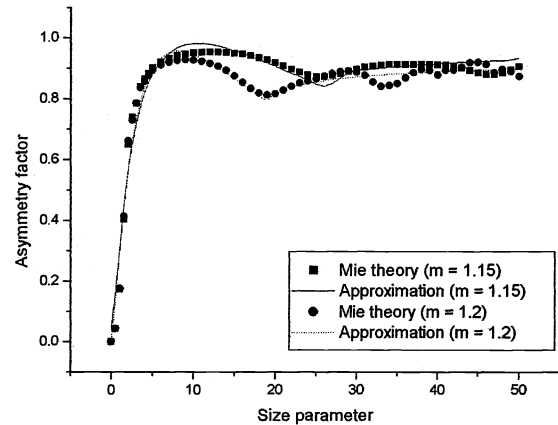


Figure 7. Average cosine of the scattering angle g for Mie scattering of non absorbing spheres as a function of size parameter x and relative refractive index m (symbols). The solid and dashed curves represent the predictions of Eqs. 3 and 4.

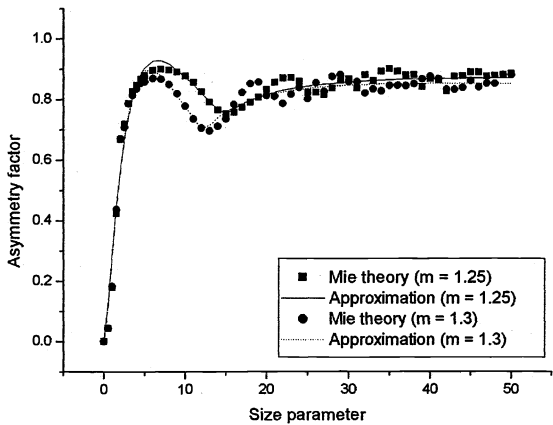


Figure 8. Average cosine of the scattering angle g for Mie scattering of non absorbing spheres as a function of size parameter x and relative refractive index m (symbols). The solid and dashed curves represent the predictions of Eqs. 3 and 4.

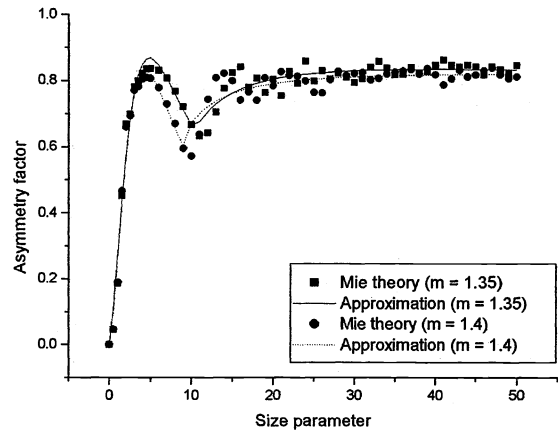


Figure 9. Average cosine of the scattering angle g for Mie scattering of non absorbing spheres as a function of size parameter x and relative refractive index m (symbols). The solid and dashed curves represent the predictions of Eqs. 3 and 4.

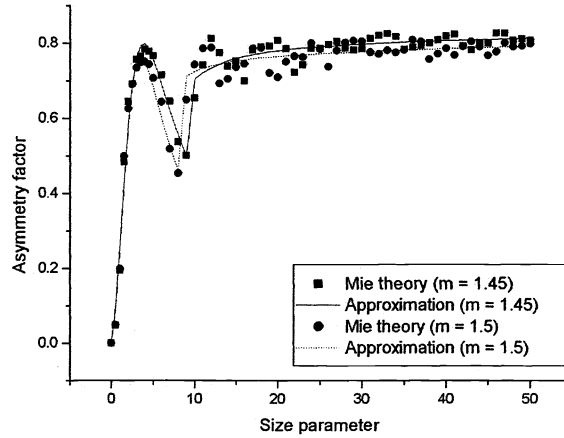


Figure 10. Average cosine of the scattering angle g for Mie scattering of non absorbing spheres as a function of size parameter x and relative refractive index m (symbols). The solid and dashed curves represent the predictions of Eqs. 3 and 4.

3.2 Approximation for case of the single infinite cylinder

3.2.1 Efficiency factor of scattering for single infinite cylinder

Figs. 11-15 present the comparison of rigorous Mie calculation and approximation offered by us (Eqs. 5, 6) for the case of scattering particles with the shape of infinite cylinder illuminated on a normal to it by non polarized light. It is seen from Figs. 11-15 that approximating formulas describe the efficiency factor behavior very well.

For x from 0 to $\frac{1}{-0.0074728439 + 0.56203885 \cdot \log(m)}$,

$$Q_{sca}(m, x) = A + B \cdot \cos(Cx + D) \quad (5)$$

where

$$A = \exp\left(1.9072955 - \frac{1.3778556}{m} - 0.74450411 \cdot \log(m)\right)$$

$$B = \frac{1}{0.97773237 - 0.5859817m + 0.17948896m^2}$$

$$C = -1.5215762 + 1.3884293m + 0.13438843m^2$$

$$D = 6.6994462 - 22.988427m + 17.952528m^2 - 4.6851572m^3$$

For x from $\frac{1}{-0.0074728439 + 0.56203885 \cdot \log(m)}$ to 50

$$Q_s(m, x) = A \exp(-Bx) \cdot \sin(Cmx + D) + E \quad (6)$$

where

$$A = \frac{1}{0.77994411m - 0.32647068}$$

$$B = \frac{-0.0060069511 + 0.0076410481m}{1 - 1.5210121m + 0.67010083m^2}$$

$$C = 0.58327399 + 0.33277931m - \frac{0.93350861}{m^2}$$

$$D = \frac{5.03830014 \cdot 10^{-4} + 4.1867205 \cdot m^{-77.992253}}{0.00012918501 + m^{-77.992253}}$$

$$E = \frac{0.11916376 + 4.2996553m}{1 + 0.61558174m + 0.51858216m^2}$$

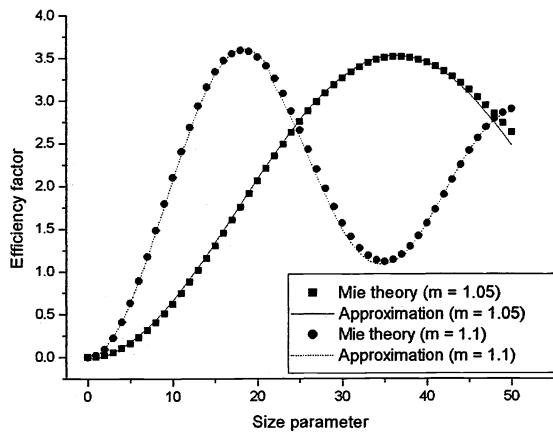


Figure 11. Efficiency factor for Mie scattering of non absorbing infinite cylinders as a function of size parameter x and relative refractive index m (symbols). The solid and dashed curves represent the predictions of Eqs. 5 and 6.

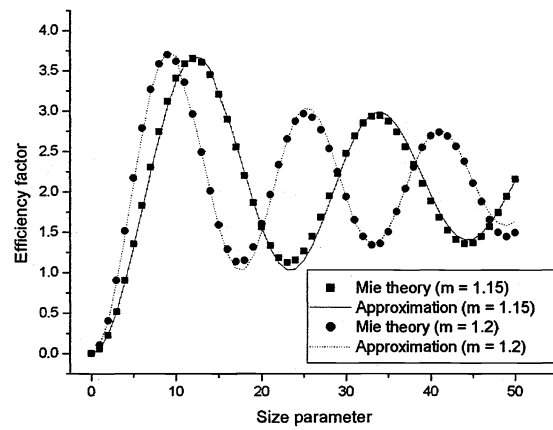


Figure 12. Efficiency factor for Mie scattering of non absorbing infinite cylinders as a function of size parameter x and relative refractive index m (symbols). The solid and dashed curves represent the predictions of Eqs. 5 and 6.

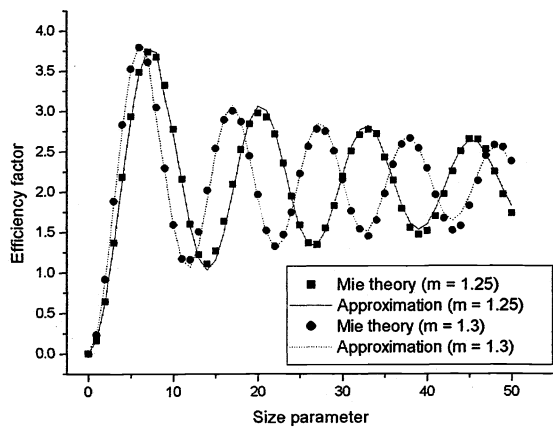


Figure 13. Efficiency factor for Mie scattering of non absorbing infinite cylinders as a function of size parameter x and relative refractive index m (symbols). The solid and dashed curves represent the predictions of Eqs. 5 and 6.

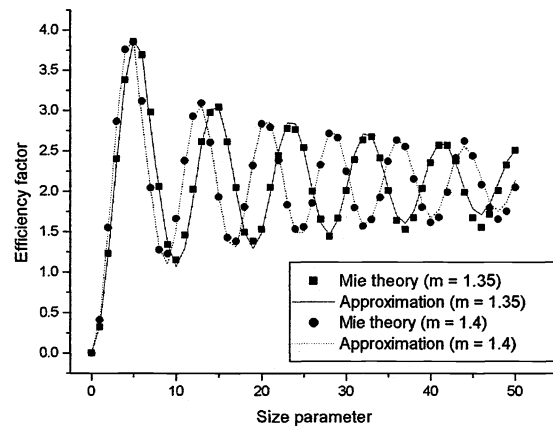


Figure 14. Efficiency factor for Mie scattering of non absorbing infinite cylinders as a function of size parameter x and relative refractive index m (symbols). The solid and dashed curves represent the predictions of Eqs. 5 and 6.

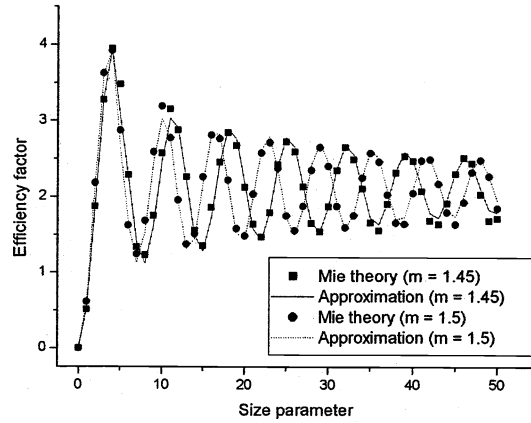


Figure 15. Efficiency factor for Mie scattering of non absorbing infinite cylinders as a function of size parameter x and relative refractive index m (symbols). The solid and dashed curves represent the predictions of Eqs. 5 and 6.

3.2.2 Asymmetry factor of single infinite cylinder

As well as for approximation of asymmetry factor for spherical particle, approximation of asymmetry factor of infinite cylinder result in less precise data in comparison with those of efficiency factor of scattering. The results of calculations of the asymmetry factor by using Mie theory and approximation offered by us (Eqs. 7, 8) are presented in Fig. 16-20.

For x from 0 to $\frac{1}{0.50696001 - 0.92345444m + 0.45971355 \cdot m^2}$

$$g(m, x) = \frac{A + Bx}{1 + Cx + Dx^2} \quad (7)$$

where

$$A = \frac{-6.67574746 - 0.0059443792 \cdot m^{16.957236}}{169.68962 + m^{16.957236}}$$

$$B = \frac{4.03569434 \cdot 10^{-3} + 0.57134927 \cdot m^{-17.3942}}{0.017951691 + m^{-17.3942}}$$

$$C = \frac{-0.01070544 + 0.41723679 \cdot m^{-14.536977}}{0.027340254 + m^{-14.536977}}$$

$$D = -0.71185255 + 0.47333509m + \frac{0.24745193}{m^2}$$

For x ranged from $\frac{1}{0.50696001 - 0.92345444m + 0.45971355 \cdot m^2}$ to 50

$$g(m, x) = A + Bx + \frac{C}{x^2} \quad (8)$$

where

$$A = \frac{-4.07622642 \cdot 10^{-3} + 0.98853994 \cdot m^{-40.215442}}{-0.0064333684 + m^{-40.215442}} + 0.0073715434 -$$

$$0.016716057 \cdot \cos(27.966678m + 0.2703813)$$

$$B = 5.8635545 - 24.754781m + 41.600981m^2 - 34.741271m^3 + 14.404556m^4 -$$

$$2.3709316m^5 - \frac{-0.010044072 + 0.0064040794m}{1 - 14.605141m + 12.139718m^2}$$

$$C = \frac{0.12614011 - 33.993243m^{-32.526833}}{-0.011909613 + m^{-32.526833}}$$

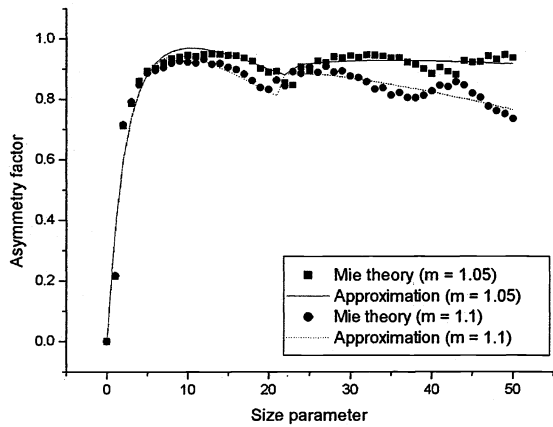


Figure 16. Average cosine of the scattering angle g for Mie scattering of non absorbing spheres as a function of size parameter x and relative refractive index m (symbols). The solid and dashed curves represent the predictions of Eqs. 7 and 8.

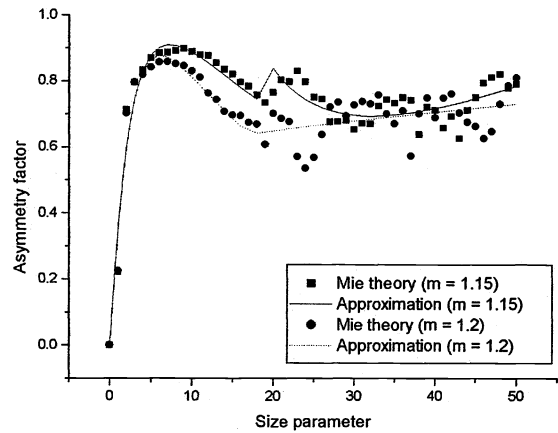


Figure 17. Average cosine of the scattering angle g for Mie scattering of non absorbing spheres as a function of size parameter x and relative refractive index m (symbols). The solid and dashed curves represent the predictions of Eqs. 7 and 8.

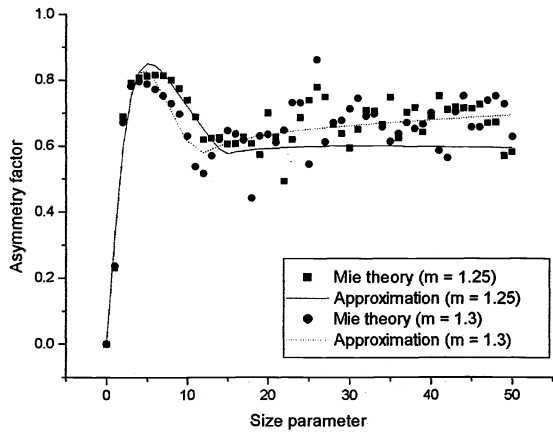


Figure 18. Average cosine of the scattering angle g for Mie scattering of non absorbing spheres as a function of size parameter x and relative refractive index m (symbols). The solid and dashed curves represent the predictions of Eqs. 7 and 8.

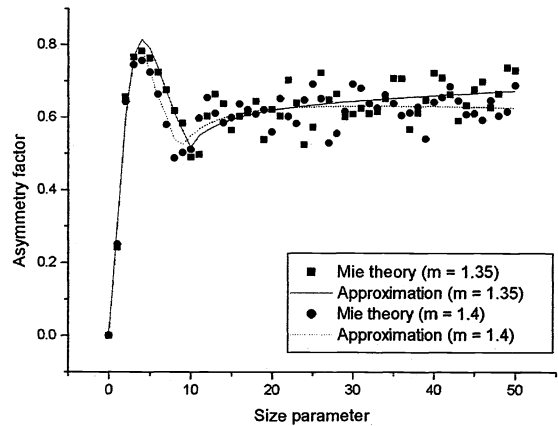


Figure 19. Average cosine of the scattering angle g for Mie scattering of non absorbing spheres as a function of size parameter x and relative refractive index m (symbols). The solid and dashed curves represent the predictions of Eqs. 7 and 8.

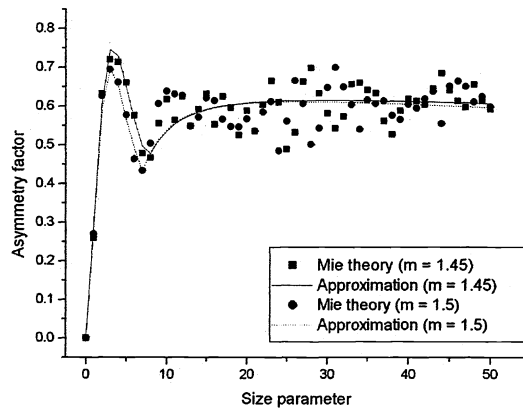


Figure 20. Average cosine of the scattering angle g for Mie scattering of non absorbing spheres as a function of size parameter x and relative refractive index m (symbols). The solid and dashed curves represent the predictions of Eqs. 7 and 8.

ACKNOWLEDGEMENTS

The research described in this publication was made possible in part by Award "Leading Scientific Schools" number 00-15-96667 of the Russian Basic Research Foundation and by Award No. REC-006 of the U.S. Civilian Research & Development Foundation for the Independent States of the Former Soviet Union (CRDF).

REFERENCES

1. M.H. Eddowes, T.N. Mills, D.T. Delpy, "Monte Carlo simulations of coherent backscatter for identification of the optical coefficients of biological tissues in vitro," *Appl. Opt.* **34**(13), pp. 2261-2267, 1995.
2. M. Hammer, A. Roggan, D. Schweitzer, G. Muller, "Optical properties of ocular fundus tissues – an *in vitro* study using the double-integrating-sphere technique and inverse Monte Carlo simulation," *Phys. Med. Biol.* **40**, pp. 963-978, 1995.
3. J.S. Dam, P.E. Andersen, T. Dalgaard, P.E. Fabricius, "Determination of tissue optical properties from diffuse reflectance profiles by multivariate calibration," *Appl. Opt.* **37**(4), pp. 772-778, 1998.
4. S.A. Prahl, *Light transport in tissue*, Ph.D. dissertation, Univ. Texas at Austin, 1988.
5. C.F. Bohren and D.R. Huffman, *Absorption and Scattering of Light by Small Particles*, Wiley, New York, 1983.
6. R.L. McCally, R.A. Farrell, "Light scattering from cornea and corneal transparency," *Noninvasive Diagnostic Techniques in Ophthalmology* / Ed. B. Masters, New York, Springer-Verlag, pp. 189-210, 1990.
7. V.V. Tuchin, I.L. Maksimova, D.A. Zimnyakov, I.L. Kon, A.H. Mavlutov, A.A. Mishin, "Light propagation in tissues with controlled optical properties," *J. Biomed. Opt.* **2**(4), pp. 401-417, 1997.